Positive$\{hk.l\}$ and negative$\{hk.\bar{l}\}$ forms of calcite (CaCO₃) crystal. New open questions from the evaluation of their surface energies.

D. Aquilano,[1] R.Benages–Vilau,[2] M. Bruno,[1] M. Rubbo,[1] F. R. Massaro[1]

[1] Dipartimento di Scienze della Terra, Università degli Studi di Torino, via Valperga Caluso 35, 10125 - Torino, Italy.

[2] Departament de Cristal·lografia, Mineralogia i DipòsitsMinerals, Facultat de Geologia, Universitat de Barcelona (UB), C/Martí i Franquès s/n, 08028 Barcelona, Spain

Summary: The surface profiles of the usually neglected negative $\{hk.\bar{l}\}$ forms of calcite are investigated, for the first time, and compared to those of the corresponding and well known positive ones: {10.4}, {01.2}, {01.8} and {21.4}. The approach combines the periodic bond chains (PBC) analysis by Hartman-Perdok (HP) that allows to build the optimal surfaces for a given crystal structure followed bythe calculation of the surface energy. The athermal equilibrium shape (at $T = 0K$), calculated for the relaxed surfaces, shows that the cleavage {10.4} rhombohedron is the most stable form of the crystal. Among the negative forms, only the steep rhombohedron $\{01.\bar{2}\}$ has a surface energy close to that of {01.2} and could compose the crystal equilibrium shape in particular environments. The growth shape calculated by the Bravais–Friedel–Donnay–Harker's (BFDH) reticular approach does not account for the properties of crystal surfaces.

1. Introduction

Calcite (space group R$\bar{3}$c, a_0 = 4.9896Å, c_0 = 17.06 Å) is the most stable (at room temperature and pressure) among the $CaCO_3$ polymorphs (vaterite, aragonite and calcite). The richness of its growth morphology is impressive: if one refers to the classical mineralogical Atlas and Handbooks, like those by Goldschmidt,[1] Dana[2] and Hintze,[3] one discovers that the number of the most recurrent {hk.l} crystallographic forms in nature is close to 150, while the total amount of the rare and/or not surely indexed ones is not far from 400. In view of such a complexity, it is somewhat surprising that scant work has been paid to the relationships between growth morphology and crystallization conditions in nature. As a matter of fact, the Kalb's[4] and Sunagawa's[5] papers represent a pioneering trial of finding a link between the growth habit and the crystallization temperature, but they were carried out before the modern theories on crystal growth had seen the light of day. Concerning the crystallization of calcite under controlled temperature, supersaturation, pH, impurity concentration, a wide literature has been produced since the sound papers of the Nielsen's[6] and Mullin's Schools,[7] who built the experimental and theoretical fundamentals for nucleation and growth kinetics of sparingly soluble salts. However, in spite of the importance of the growth morphology of the $CaCO_3$ polymorphs in both applied and theoretical problems (e.g., biomineralization) the first rigorous paper on the relationship between growth morphology and crystal structure of calcite appeared in 1985 by Heijnen,[8] who found a reasonable correlation between the observed morphology of gel grown crystals and the theoretical growth morphology, analysed in the light of the Hartman-Perdok theory.[9] According to Heijnen's calculations, limited to the interaction among first neighbours, only two rhombohedra, {10.4} and {01.2} show flat (F) character, while the prism {11.0} is a stepped forms; any other {hk.l} form was considered.

In the last 25 years a lot of papers has been published on the morphology/structure relationship and surface and attachment energy evaluations of "low indexes" forms have been carried out with the aim at predicting both theoretical equilibrium and growth morphologies of calcite. Very recently, we published an exhaustive paper on this topics[10] where, in the section on the free energy of the main calcite/water interfaces, we outlined the wide dispersion of experimental and theoretical data on both dry and wetted surfaces existing in nowadays literature.

Furthermore, it is worth considering that nothing has been done for predicting the morphological importance (MI) of the negative {$hk.\bar{l}$} forms of calcite (compared to the corresponding {$hk.l$} positive ones), even if their MI should not be negligible as it follows, for instance, from the observed occurrence frequency (1.8%) of the {10.$\bar{4}$} form, compared to that (35.8%) of the more famous cleavage {10.4} rhombohedron.[1-3]

The theoretical equilibrium shape (ES) of a crystal is unique since, at given temperature and pressure, it only depends on a thermodynamic property, i.e. on the ratio among the specific surface energies (γ_{hkl}) of the different {hkl} forms. Hence, predicting the ES of a crystal can be reduced to calculate the γ_{hkl} values, without or in the presence of foreign adsorption (solvent and/or impurities). On the contrary, the theoretical growth morphology of a crystal cannot be unique, because it depends on the growth mechanisms of the different {hkl} forms which, in turn, depend on: i) the character of the forms, ii) the supersaturation of the mother phase, iii) the adsorption kinetics, if any, iv) the number and activity of the dislocations outcropping the growing crystal surfaces and, finally, v) the fluid-dynamics of the surrounding growth medium. It turns out that predicting the growth shape (GS) is much more complicated than the approach to the ES, and hence only approximated evaluations have been attempted in the past. In short, there are two historical paths of predicting the growth morphology of crystals, starting from the knowledge of their bulk structure.

The first one, proposed as the Bravais-Friedel law[11] and improved by Donnay-Harker (BFDH),[12] states that higher the equidistance d_{hkl}, higher the MI of the {hkl} form. The d_{hkl} spacing has to fulfil the systematic extinction rules, owing to the space group glide operations and centring of the non-primitive lattice types. According to a limited number of examples examined by Hartman,[13] the correspondence between the MI of a crystal form and its d_{hkl} value should be rather good; then, there must be a physical basis behind this geometrical-reticular way of thinking. As a matter of fact, d_{hkl} represents the period (or the pseudo-period) with which the surface energy is repeated and, in the case of the flat faces, d_{hkl} is nothing else that the thickness of the elementary growth layer. On the other hand, from the BFDH criterion one could argue that two {$h_1k_1l_1$} and {$h_2k_2l_2$} forms corresponding to two equivalent spacing d($h_1k_1l_1$) = d($h_2k_2l_2$), should show the same MI index. Furthermore, two iso-structural crystals, such as calcite ($CaCO_3$) and nitratine ($NaNO_3$), should have the same theoretical growth shape: actually, the growth morphology of calcite is extraordinarily rich, whilst that of nitratine is very poor. Many unambiguous examples proved that the BFDH approach is not always reliable, but this should not be surprising since nowadays it is well known that the MI of a crystal form does depend not only on structural factors, but from surface energetic and kinetics and, finally, on the interactions with the surrounding phase. Nevertheless, the BFDH approach is still widely used.

The second method for predicting crystal morphologies was formulated by Hartman and Perdok (HP hereinafter) fifty years ago and successively implemented.[9] This approach is grounded on the idea that the advancement rate (R_{hkl}) of a (hkl) face is proportional to its attachment energy E_{hkl}^{att}, i.e. the energy released, per formula unit, when a d_{hkl} layer attaches on the pre-existing substrate

4

during growth. In other words, higher the E_{hkl}^{att} value, higher the corresponding R_{hkl} and, consequently, lower the MI of the corresponding form. An unavoidable step, in evaluating E_{hkl}^{att}, is the preliminary choice of the surface profile on which the d_{hkl} layer attaches. In fact, the profile is not necessarily unique and then the most reasonable choice is that corresponding to the profile showing the lowest surface energy value (γ_{hkl}^{min}). The surface profiles can be obtained, from structural data, by rigorously applying the HP rules for finding the periodic bond chains (PBCs) in the crystal structure and then the character of the crystal faces: flat (F), stepped (S) and K (kinked). With the aid of the HP method one can foresee the morphology and also the habit of a crystal, even if one does not consider either the effect of the supersaturation, or the differences introduced in the growth rate of the faces by the activity of the screw dislocations. Moreover, the comparison among the different E_{hkl}^{att} values cannot consider that the solvent and impurity adsorption plays different roles on the different crystal forms. Nevertheless, the following reasons prove that the properties of the HP method are relevant:

- even if more sophisticated[14] or computerized[15] methods have been proposed to solve the problem of finding the "best surface profiles", the HP analysis results to be the most reliable one, as much as the complexity of the crystal structure increases;

- a coherent reconstruction of the dipolar surfaces can be obtained "only" by applying the PBC analysis, since it intrinsically fulfils the symmetry conditions imposed by the crystal bulk;[16-20]

- finding the best surface profiles is a prerequisite for calculating the adhesion energy of twinned and epitaxial layers and for simulating both random and organized adsorption of any foreign phase onto a crystalline substrate (i.e. molecular dynamics simulations).[21-28]

In this paper:

- first, we will predict the theoretical GS of calcite by applying the BFDH approach and compare our results with the occurrence frequency of the natural calcite {$hk.l$} forms;

- secondly, we will extend the investigation to the surface profile of the negative {$hk.\bar{l}$} forms of calcite, following the HP approach, and focus our attention to their specific surface energies. This, in order to compare their equilibrium properties with those of the positive {$hk.l$} ones and find if some of them can compose the ES of the crystal.

It will be confirmed that the BFDH approach is weaker with respect to the HP one, especially when dealing with a crystal like calcite in which the simplicity of the structure (very similar to that of the NaCl – lattice type) is coupled with the strong anisotropy introduced by the geometry of the carbonate ion. It will be also demonstrated that the rich growth morphology of calcite has its own

reason of existence on the athermal equilibrium shape (ES) of calcite (i.e. the relaxed one calculated at 0K), even if the solvent (water) adsorption is not considered. As a matter of fact, it will be shown that, contrary to what is commonly believed, the theoretical ES of calcite is richer in crystallographic forms with respect to the corresponding theoretical growth shape (GS), which is drawn from the E_{hkl}^{att} values.

All over the paper we will adopt, for the sake of simplicity, the short notation for the indexes: *hk.l* instead of *hkil* where $i = -(h+k)$, as usually done for both trigonal and hexagonal symmetry systems. Besides, we describe with an example what we mean with the term "occurrence frequency of a given {*hk.l*} form". Let's consider a population of thousand crystals grown under different natural or laboratory environments; if a {*hk.l*} form is found to occur, either alone or combined with other forms, on 350 crystals, then its occurrence frequency will be 35%. This is the meaning of "occurrence frequency" (or Fundortpersistenz, in German) which is commonly used in the classical Handbooks of Mineralogy.

2. TheBFDH approach to the growth form of calcite

The MI of the calcite forms are evaluated by calculating the $(d_{hk.l})^{-1}$ values and drawing the corresponding Wulff's plot,[29] the minimum among these values being assumed as a reference one. Hence, the theoretical growth shape is built, according to the BFDH method, by considering only those spacing that fulfil the systematic extinction rules of calcite space group, $R\bar{3}c$ (see Fig. 1). It is worth mentioning that the d_{hkl} values (satisfying the diffraction Bragg's law) and the surface profiles of the {*hkl*} forms only share the position of the geometrical *hkl* plane: as a matter of fact, it may happen that $d_{hkl} = d_{h'k'l'}$, while the surface profile of the face (*hkl*) is completely different from that of the (*h'k'l'*) one. Moreover, in the case of calcite, it is plain that $d_{hk.l}$ and $d_{hk.\bar{l}}$ do fulfil the same extinction rule, while the surface profiles of the corresponding forms should be quite different.

FIGURE 1

Table 1. Lattice spacing of calcite crystal (column 2) calculated according to the systematic extinction rules. The observed occurrence frequency of the crystal forms are reported in column 5.

Form {hk.l}	d_{hkl} (Å)	$(d_{hkl})^{-1}$ (Å)$^{-1}$	Ratio to the minimum $(d_{hkl})^{-1}$ value	Observed * occurrence frequency (%)	Rank* of the observed Morphological Importance (MI)
{01.2}	$d_{01.2} = 3.8555$	0.25937	1.0000	24.2	5
{10.4}	$d_{10.4} = 3.0364$	0.32934	1.2697	35.7	4
{00.1}	$d_{00.6} = 2.8448$	0.35152	1.3552	17.2	7
{11.0}	$d_{11.0} = 2.4951$	0.40078	1.5452	14.1	8
{11.3}	$d_{11.3} = 2.2850$	0.43763	1.6873	–	–
{10.1}	$d_{20.2} = 2.0947$	0.47739	1.8406	23.8	6
{01.8}	$d_{01.8} = 1.9132$	0.52268	2.0152	37.2	3
{11.6}	$d_{11.6} = 1.8758$	0.53310	2.0553	–	–
{21.1}	$d_{21.1} = 1.6260$	0.61500	2.3711	–	–
{12.2}	$d_{11.2} = 1.6043$	0.62332	2.4032	–	–
{21.4}	$d_{21.4} = 1.5255$	0.65552	2.5273	38.9	2
{11.9}	$d_{11.9} = 1.5099$	0.66229	2.5534	–	–
{12.5}	$d_{12.5} = 1.4734$	0.6787	2.6167	–	–
{10.0}	$d_{30.0} = 1.4405$	0.69420	2.6765	46.3	1

*Unpublished data obtained from a classification of near 3000 natural growth forms drawn in the reviews cited in ref. [1-3]

Three considerations come out:

(i) The positive steep {01.2} rhombohedron and its corresponding negative one {01.$\bar{2}$} are the dominant forms, both showing the same MI, owing to the fact that the BFDH criterion "artificially" introduces the equatorial 00.1 symmetry plane. A third form, the {00.1} pinacoid, truncates the two steep rhombohedra, while the {10.4} rhombohedron does not appear at all (neither positive nor negative). This does not agree with the observed ranking of the growth morphology. In fact, from a careful investigation on an extremely wide collection[1-3] (close to 3000 natural samples), we found that the three most important forms are the prism {10.0}, the scalenohedron {21.4} and the flat rhombohedron {01.8}, while the {01.2}, {10.4} and {00.1} forms occupy only the fifth, the fourth and the seventh position, respectively (Table 1, column 6).

(ii) The BFDH growth shape is a "static" one, in the sense that it is built only from reticular data and hence cannot be modified by adding neither lattice energies nor thermodynamic (surface entropy contributions, solvent adsorption) and kinetic effects (like the attachment energy of the growth units to the face which is proportional to its advancement rate).

(iii) These discrepancies are not so surprising since a criterion based on the lattice plane spacing cannot take into account the strong anisotropy that characterizes the calcite structure in which spherical ions (Ca^{2+}) coexist with triangular ones (CO_3^{2-}) giving rise to sensible differences in the surfaces profiles of the crystal slices having the same thickness but different crystallographic orientation.

3. Computational details

Calculations (optimizations of slab geometries, and surface and attachment energies) were performed by using the inter-atomic potential for calcite developed by Rohlet al.[30] (Rohl potential hereinafter) and the General Utility Lattice Program (GULP) simulation code[31] which, being based on force field methods, allows the calculation of structures and properties of minerals from a given set of empirical potentials. Geometry optimization is considered converged when the gradient and the function tolerance (*gtol* and *ftol* adimensional parameters in GULP) are smaller than 0.0001 and 0.00001, respectively.

The surfaces were studied by using the 2D-slab model.[32] The slabs of varying thickness were generated by separating the bulk structure along the plane of interest.

The geometry optimization was performed by means of the Newton-Raphson method and by considering the slab subdivided into two regions: region 1, which contains both the surface and the underlying atomic layers that are allowed to relax, and region 2 which has the same number of layers of the region 1, and contains the rest of the slab material where no relaxation with respect to the bulk crystal structure is assumed to occur.

Calculations were done by considering slabs with thickness up to ten layers (in both the regions 1 and 2), which are sufficient to reproduce bulk-like properties at the center of the slab and to obtain a careful description of the surface. According to the standard two-regions strategy employed by GULP, the specific surface energy (γ, erg/cm^2) was evaluated from the energy of the surface block (U_s, region 1) and the energy of a portion of bulk crystal (U_b) containing the same number of atoms as the surface block. Both energies have been referred to *A,* the common surface area of the primitive unit cell:

$$\gamma = \frac{U_s - U_b}{A} \quad (1)$$

A ten layer slab (in both the regions 1 and 2) was sufficient to reach convergence on the γ values. The attachment energy E_{hkl}^{att} is given by:

$$E_{hkl}^{att} = U_{tot}^{n+1} - U_{tot}^{n} - U_{lc}^{1} \qquad (2)$$

where U_{tot}^{n} represents the total internal energy of a surface model consisting of n growth layers, and U_{tot}^{1} is the energy of the growth layer alone. In practice, the calculation of this exothermic quantity is obtained from the interaction energy of anelementary growth layer at the crystal surface with the rest of the underlying material.

4. A comparison between the character (HP method) of positive and negative forms of calcite. The corresponding surface profiles and specific surface energies

4.1. The positive $\{10.4\}$ (cleavage) and negative $\{10.\overline{4}\}$ rhombohedra

Let's consider the projection of calcite structure along one out of the three equivalent <100> directions and examine the $\{10.4\}$ and $\{10.\overline{4}\}$ unrelaxed forms that are illustrated in Fig. 2 with their surface profiles exposed to the vacuum. As we demonstrated in a preceding paper,[33] the $\{10.4\}$ cleavage rhombohedron shows a marked F character, since more than two strong different PBCs run within a slice of thickness $d_{10.4}$. This slice is not dipolar (no electric dipole moment perpendicular to its surface): in fact, the centres of mass of both positive and negative ions are situated on a unique plane lying midway of the slice. Consequently, the separation planes between successive $d_{10.4}$ slices do not intercept the centre of mass of any ion.

From the distribution of the electrical charges in the $d_{10.\overline{4}}$ slice, a completely different situation sets in its surface profile. Also this slice is not dipolar, even if the centres of mass of the opposite ions do no longer lye on a unique plane; in fact, they are distributed on four successive planes, within the slice thickness, each plane containing an equal density of opposite charges (see Electronic Supplementary Information, ESI, Fig. S1). Another important feature makes the difference between the $\{10.4\}$ and $\{10.\overline{4}\}$ forms. At variance with the cleavage rhombohedron, the adjacent $d_{10.\overline{4}}$ slices share the separation planes: it follows that also the charges lying on the dividing plane should be partitioned alternately to a slice and to the adjacent one. In other words, their site occupancy is only ½ and hence the repeat period of every ion belonging to a separation plane is no longer the unit cell

vector [100], but [200]. This implies that the structure of the <100> PBCs running within a $d_{10.\bar{4}}$ slice should be weaker than that of the corresponding one in the $d_{10.4}$ slice. Having also considered that another weak PBC develops in the $d_{10.\bar{4}}$ slice and bounds the <100> PBCs, the resulting F character of the $\{10.\bar{4}\}$ forms is necessarily weaker than that of the positive $\{10.4\}$ form. Moreover, also the $\{10.\bar{4}\}$ surface profile is unique, but this analysis indicates that $\{10.\bar{4}\}$ should be much less stable than the cleavage rhombohedron. At last, the $\{10.\bar{4}\}$ surface profile results to be composed of nano-facets, a case similar to the $\{21.4\}$ scalenohedron, as we will see later on.

A dramatic consequence follows: relaxation practically does not affect the $\{10.4\}$ surface configuration, whilst an important change of coordination occurs in the outmost three layers of the $\{10.\bar{4}\}$ surface. The relaxed surface energy differs as much as $\Delta\gamma_{relaxed}$ = +104 % , being $\gamma_{relaxed}^{10.4}$ = 534^{22} and $\gamma_{relaxed}^{10.\bar{4}}$ = 1087 erg cm^{-2}. Actually, one ought to have expected such a sharp difference between these opposite rhombohedra. As a matter of fact, the $d_{10.\bar{4}}$ slices are practically perpendicular to the $d_{10.4}$ ones, as it can be found in the ESI (Fig. S1) where the calculated angle between the two faces is 89.25°. The meaning of this pseudo-orthogonal orientation is well over the pure geometry: we would like remembering that the excellent cleavage property of the $\{10.4\}$ form is strictly related to its relaxed surface energy (as it comes out from the cleavage energy definition): $\gamma_{relaxed}^{10.4}$ = 534 erg cm^{-2}, that represents the minimum among the relaxed surface energies of calcite.[22]

Hence, it is easy understanding that the flat $d_{10.\bar{4}}$ slice, which is orthogonal to the perfect cleavage surface, should be associated to the maximum of the relaxed surface energy. In fact, it is not by chance that $\gamma_{relaxed}^{10.\bar{4}}$ = 1087 erg cm^{-2}.

4.2. The positive $\{01.8\}$ and negative $\{01.\bar{8}\}$ flat rhombohedra

The flat $\{01.8\}$ rhombohedron shows a marked S character[34] since no bonds can be found between the $<\bar{4}\,41>$ PBCs, which are the only ones running within the allowed $d_{01.8}$ slices. Also this slice is not dipolar, like the one having the $d_{10.4}$ thickness; moreover, also in this case the centres of mass of both positive and negative charges lie midway of the slice (see ESI, Fig. S2).

The $\{01.\bar{8}\}$ form shows a quite different surface structure. The S character is preserved: within the $d_{01.\bar{8}}$ slices, complex and polar <100> develop but the symmetry centre cancels out the polarity of the slices. As for the $\{10.\bar{4}\}$ rhombohedron, two important features characterize the $\{01.\bar{8}\}$ form:

(i) the electrical charges are distributed in the slice on four successive and parallel planes, each plane being electrically neutral;

10

(ii) the adjacent $d_{01.\bar{8}}$ slices are separated by "frontier planes" belonging to both a slice and to the adjacent one: hence, the ions lying on the frontiers should have an occupancy of only one half. In this connection, we would like to say that the occupancy of half sites on the frontier planes between two adjacent slices is not dictated by computational constraints; on the contrary, the distribution of the occupied sites should respect the 2D symmetry of the frontier plane and fulfil both the stoichiometry and the surface periodicity of the slice, ultimately, in order to set an initial surface configuration to start to minimize the energy of the face parallel to the slice.

From Fig. 2 one can see that the surface relaxation blurs the distinction between the unrelaxed and the relaxed profile of {01.8} and {01.$\bar{8}$} forms, at variance with what occurs for the cleavage and the {10.$\bar{4}$} rhombohedron. Hence, the difference in the surface energy values is not dramatic: in fact, it increases by +15.4%, varying from $\gamma^{01.8}_{relaxed} = 702$[35] to $\gamma^{01.\bar{8}}_{relaxed} = 810$ erg cm^{-2}.

4.3. The positive {21.4} and negative {21.$\bar{4}$} scalenohedra

The {21.4} scalenohedron has more or less the same natural occurrence frequency of the flat {01.8} rhombohedron (Table 1). Moreover, the scalenohedron is the typical form of calcite in the precipitated calcium carbonate particles (PCC) that are used as fillers or pigments in plastics, paper, food and pharmaceutical industrial fields.[36] Its character is stepped (S), since no bonds can be found between adjacent <$\bar{4}$41> PBCs within a slice of thickness $d_{21.\bar{4}}$; hence, also this form cannot grow by lateral spreading of $d_{21.\bar{4}}$ mono-layers. To find a correlated growth among the <$\bar{4}$41> chains one has to consider a slice of double thickness. In this case, the resulting wavy surface profile (Fig. 2) is the most stable one and can be imagined as composed by alternating segments of {10.4} and {11.0} nano-facets having the length of 0.315 and 0.382 nm, respectively (the alternating segments appearing in Fig. 2 are clearly drawn, in detail, in the ESI, Fig. S3top). The strongest δ_1, δ_2 and δ_3 bonds link the <$\bar{4}$41> chains within the {10.4}nano-segments, while the {11.0} ones are built by the weaker δ_4 bonds.[35]

The complex slice structure of the {21.$\bar{4}$} scalenohedron is illustrated in detail in the ESI; here we confine our attention to the corresponding surface structure. It is quite worth comparing the relaxed profiles of positive and negative scalenohedra. The positive one preserves the wavy profile of the un-relaxed structure and the structure perturbation does affect the three outmost layers; on the contrary, the six outermost surface layers of the negative scalenohedron are strongly perturbed and disordered, especially the external one which is characterized by the relaxation of the carbonate ions that change their orientation from quasi-vertical to quasi-horizontal and parallel to the face plane.

The increase ofthe relaxed surface energy from $\{21.4\}$ to $\{21.\bar{4}\}$ scalenohedron is higher with respect to that of the flat rhombohedron, being $\gamma_{relaxed}^{21.4} = 783^{35}$ and $\gamma_{relaxed}^{21.\bar{4}} = 858$ erg cm^{-2}, which implies a relative difference $\Delta\gamma_{relaxed} = + 22.35$ %.

4.4. The positive $\{01.2\}$ and negative $\{01.\bar{2}\}$ steep rhombohedra

The surface structure of positive $\{01.2\}$ steep rhombohedron has been extensively studied[16] and the surface energies of the related surface profiles have been determined as well.[16,18] Here we deal with a F form, since three PBCs ($<100>$, $<42\bar{1}>$ and $<211>$) run within the allowed d$_{012}$ slice. However, the peculiarity of this form is that is intrinsically dipolar, owing to the sequence of crystallographic 01.2 planes populated by alternating Ca^{2+} and CO_3^{2-} ions. In detail, a d$_{01.2}$ slice is limited by two external Ca^{2+} planes which are separated by a CO_3^{2-} plane; obviously, the complementary distribution exists as well (external CO_3^{2-} planes which are separated by a Ca^{2+} plane). Hence a surface reconstruction is needed, in order to cancel out the electrical dipole moment perpendicular to the face. This complex operation can be performed in different ways;[16,18] here we recollected only four of them, grounded on the PBC method, from which the surface profile with minimum surface energy is obtained (see ESI, Fig. S4). As a matter of fact, two out of the four reconstructed profiles respect the symmetry of the crystal bulk; moreover, one of them is Ca^{2+} terminated while the other one is terminated with the carbonate ions. This last profile, drawn in Fig. 2 for both unrelaxed and relaxed surface, is associated to the minimum surface energy[18] ($\gamma_{relaxed}^{01.2} =$ 750 erg cm^{-2}), the relaxation reducing the $\gamma_{01.2}$ value by near 5 times with respect to the unrelaxed profile. It is worth remembering that the peculiar feature of this minimum energy surface is determined by the fact that the outmost CO_3^{2-} layer of the reconstructed $\{01.2\}$ form has a coverage degree of one half, owing to the structure of the $<100>$ PBCs that show a repeat period of $|<200>| = 9.978$ Å.

The slices of the negative steep $\{01.\bar{2}\}$ rhombohedron, of thickness $d_{01.\bar{2}}$, are also intrinsically dipolar, being built by alternating planes of Ca^{2+} and CO_3^{2-} ions. Unlike the d$_{01.2}$ slice, the opposite alternating ions are distributed on seven planes (two external limiting the slice, and five within it). This implies different structures of the $<100>$ PBCs and, consequently, of the surface profiles. Two examples of the reconstructed $d_{01.\bar{2}}$ slices are illustrated in detail in the ESI; also in

this case the surface profiles are characterized by an occupancy of one half the population of the outmost ions.

We confine our attention to the relaxed surfaces and to the surface termination showing the minimum energy. The calculation of the corresponding surface energies gives unexpected results: indeed it comes out that the positive[18] and the negative steep rhombohedron have a very close surface energy: $\gamma_{01.2}^{relaxed} = 750$, $\gamma_{01.\bar{2}}^{relaxed} = 718$ erg cm^{-2} and $\Delta\gamma_{relaxed} = -4.3$ %. Hence, at 0K, the negative steep rhombohedron is more stable that the positive one.

Table 2. Relaxed surface energies (γ, erg/cm^2) of the main positive $\{hk.l\}$ and the corresponding negative $\{hk.\bar{l}\}$ forms of calcite. Values of the neutral forms $\{10.0\}$, $\{00.1\}$ and $\{11.0\}$ are also given to better understand the equilibrium shape of calcite. Only the lowest surface energy value has been indicated for the crystal forms $\{01.2\}$, $\{01.\bar{2}\}$ and $\{00.1\}$ which show more than one surface termination. In the 7th column, the differences (per cent) between the values of negative and positive forms. The E_{att} values (erg/molecule $\times10^{12}$) are indicated as well; the E_{att} of the forms $\{01.2\}$, $\{01.\bar{2}\}$ and $\{00.1\}$ are missing since the calculation of the attachment energy through the method of the systematic cuts[15,37] cannot be made, owing to the reconstruction of the corresponding surface profiles.

Positive forms	$\gamma_{relaxed}$	E_{att}	Negative forms	$\gamma_{relaxed}$	E_{att}	$\Delta\gamma_{relaxed}$ (%)	Neutral forms	$\gamma_{relaxed}$	E_{att}
$\{10.4\}$	534[30]	-2.968[35]	$\{10.\bar{4}\}$	1087	-13.303	+104.0	$\{10.0\}$	722[38]	-25.681
$\{01.8\}$	702[35]	-9.718	$\{01.\bar{8}\}$	810	-21.593	+15.4	$\{00.1\}$	711[20] (CO_3^{2-} external)	
$\{21.4\}$	783[35]	-9.605	$\{21.\bar{4}\}$	958	-52.672	+22.3	$\{11.0\}$	1232[38]	-9.721[35]
$\{01.2\}$	750[18] (CO_3^{2-} external)		$\{01.\bar{2}\}$	718 (CO_3^{2-} external)		-4.3			

FIGURE 2

5. Discussion

The evaluation of the surface energy of the main negative forms leads us to revise the relative importance of the "historical" forms of calcite and allows to remove some ambiguities concerning the calcite morphology.

a) Now it is evident that one has to take the *cleavage {10.4} rhombohedron as the reference form of the calcite morphology* and we have just found why. Contrary to BFDH model that equates the morphological importance of positive $\{10.4\}$ and negative $\{10.\bar{4}\}$ rhombohedron, the dramatic

difference between their surface energies excludes the $\{10.\overline{4}\}$ form both the equilibrium and growth shape of calcite in pure medium: it is not by chance that its observed occurrence frequency barely reaches 1.8%

In fact, neither the configurational and vibrational entropic contributions nor the solvent (water) adsorption can compensate the difference of 554 erg cm^{-2} which separates the two surface profiles: consequently, only the cleavage $\{10.4\}$ form can make the equilibrium shape of the crystal, whatever the temperature of the aqueous solution surrounding it. An even more convincing argument concerns the growth form: the $\{10.\overline{4}\}$ attachment energy is four times larger than that of the $\{10.4\}$ one and hence the ratio of the (eventual) growth rates absolutely tell against the $\{10.\overline{4}\}$ form. *This means that when one observes a "classic" calcite rhombohedron grown from pure aqueous solution, this can be only the cleavage one*.

b) Apart the $\{10.0\}$ prism and the $\{00.1\}$ pinacoid, which are "neutral forms" (being neither positive or negative), the $\{01.2\}$ steep rhombohedron is the other form entering the athermal equilibrium shape of the crystal[38] which is much more faceted with respect to that usually reported in literature.

Nevertheless, the $(01.\overline{2})$ rhombohedron face, which belongs to the only negative calcite form showing a surface energy lower than that of the corresponding positive one, is pinned between two faces, $(01.\overline{2})$ and $(01.\overline{4})$, more stable in vacuum at 0K; but we cannot exclude that marginal entropic effects and adsorption determine its relative stability.

A second feature refers to the growth shape of the crystal. Let's imagine that, for some kinetic reason, the $\{10.0\}$ prism does disappear from the growth shape; remembering that the $\{00.1\}$ form does not interfere in the competition between the rhombohedra, three forms should remain to define the crystal surface: $\{10.4\}$, $\{01.2\}$ and $\{01.\overline{2}\}$. The case in which only $\{10.4\}$ survives is trivial, very usual in literature, and $\{10.4\}$ cannot be confused with the $\{10.\overline{4}\}$ form, as we just demonstrated. But also the case in which the steep rhombohedron exists alone in the growth shape has a high occurrence frequency,[16] and hence a well-founded question arises from the comparison we made between the two opposite forms: which of the two possible rhombohedra it is? This question is not a purely academic one: in fact, the steep rhombohedron is a strategic face in biomineralization experiments, along with the pinacoid $\{00.1\}$, since it is often used as a suitable template for building self- assembled molecular systems (SAMS).[39] As a consequence, one has to be cautious when choosing $\{01.2\}$ or $\{01.\overline{2}\}$ surfaces as templates, without having examined their

surface growth or dissolution figures, the only fingerprint to distinguish, for sure, the positive from negative steep rhombohedron.

FIGURE 3

6. Conclusions

By applying the Hartman-Perdok method, we proved that this approach is so versatile as to allow to understand the fundamental factors (surface and attachment energies) determining why the positive forms of calcite usually prevail on the negative ones. The surface energies at 0K of the negative forms of calcite were calculated at empirical level and compared with those of the positive ones. From the analysis of the theoretical equilibrium shape of calcite, it results that the most extended form is a non-polar F form, the cleavage $\{10.4\}$ rhombohedron, and that a polar F form, the steep rhombohedron $\{01.2\}$, along with a S form, the prism $\{10.0\}$ and a K form, the pinacoid $\{00.1\}$ make the equilibrium shape of the crystal as well. Moreover, a competition arises between the steep rhombohedra $\{01.2\}$ and $\{01.\bar{2}\}$, since the negative is more stable, at equilibrium, than the positive one; this unexpected result opens new paths for interpreting biomineralization experiments in which calcite plays a fundamental role.

We also showed that calcite is an effective litmus test to resolve an age-old problem: is the BFDH approach a good way to foresee the morphological importance of a given $\{hkl\}$ form and hence the growth shape of a crystal, as it is often used nowadays in the world of crystallography? The answer is no, even if the BFDH method maintains its historical and didactic interest. The lack of the equatorial 00.1 symmetry plane in calcite does not interfere with the fact that the spacing of the symmetry equivalent planes $d_{hk.l}$ and $d_{hk.\bar{l}}$ is be the same and hence the BFDH approach is not able to distinguish, as an example, between the morphological importance of the $\{10.4\}$ cleavage rhombohedron from that of the $\{10.\bar{4}\}$ form. In the same way, a structural crystallographer cannot distinguish, in a X-ray powder diagram, the contribution of the two plane families: 10.4 and 10.$\bar{4}$, simply because the diffraction angle $\theta_{hk.l}$ coincides with $\theta_{hk.\bar{l}}$, even if the related peak intensities necessarily differ each other.

A last comparison between BFDH and HP approach concerns the iso-structural compounds. The BFDH method cannot discriminate the morphological importance of the calcite forms from that of nitratine ($NaNO_3$). On the contrary, we would expect a marked difference between equilibrium and

growth shapes of these two substances, owing to their sharplydifferent crystal fields. This needs further investigations and will be the subject of a forthcoming paper.

Acknowledgments

Electronic Supplementary Information (ESI) Available. Projection and description of the calcite structure along the directions [010] (Figs. S1, S2 and S4), and [$\bar{4}$41] and [1$\bar{2}$0] (Fig. S3).

References

1 V. Goldschmidt, *Atlas der Krystallformen*, Carl Winters Universitätbuchhandlung, Heidelberg 1913-1923, **vol. 3b**.

2 R. V. Gaines, H. C. Skinner, E. E. Ford, B. Mason and A. Rosenzweig, *Dana's New Mineralogy,*with sections by V. T. King, Illustrations by E. Dowty, 1997, John Wiley & Sons, Inc.

3 C. A. F Hintzeandand and G. E. Linck, *Handbuch der Mineralogie*, **1st Band**, Leipzig (1897) Veit&Comp.

4 G. Kalb, *Zentralblatt Miner.*, 1929, **Abt. A4**, 137.

5 I. Sunagawa, *Rep. Geol. Surv. Japan*, 1953, **155**, 1-66 (in Japanesewith English Abstract).

6 (a) A.E. Nielsen and O. Söhnel, *J. Cryst. Growth,* 1971, **11**, 233-242; (b) A.E. Nielsen and J.M. Toft, *J. Cryst. Growth,*1984, **67**, 278-288; (c) A.E. Nielsen, *J. Cryst. Growth,*1984, **67**, 289-310.

7 (a) J.W. Mullinandand O. Söhnel, *Chem. Eng. Science*, 1977, **32**, 683-794; (b) O. Söhnelandand J.W. Mullin, *Chem. Eng. Science*, 1978, **33**, 1535-1538; (c) J. W. Mullin, *Crystallization*, 4th Ed. London, 2001, Butterworth-Heinemann.

8 W. M. M. Heijnen, *Neues Jahr. Mineral. Mon. Hefte*, 1985, **8**, 357-362.

9 (a) P. Hartman and W. G. Perdok, *Proc. Koninkl. Nederland. Akad. Wetenshap.*, 1952, **Ser. B55**, 134-136; (b) P. Hartman and W. G. Perdok, *Acta Cryst.*,1955, **8**, 49-52; ibid., 521-524; ibid., 525-529; (c) P. Hartman, in *Morphology of Crystals* part A., 1987, Ed. I. Sunagawa, Terra Sc. Publ. Comp. Tokyo, 269-319.

10 M. Bruno, F. R. Massaro, L. Pastero, E. Costa, M. Rubbo, M. Prencipe and D. Aquilano, *Cryst. Growth Des.,* 2013, **13**, 1170-1179.

11 G. Friedel, *Bull. Soc. Franc. Minér.*,1907, **30**, 326.

12(a) J. D. H. Donnay and D. Harker, *Amer. Miner.*, 1937, **22**, 446- 467; (b) J. D. H. Donnay and G. Donnay,*Compt. Rend. Acad. Sci. Paris,* 1961, **252**, 908-909.

13 P. Hartman, in *Crystal Growth: An Introduction*, 1973, Ed. P. Hartman, North Holland, Amsterdam, 367-402.

14 R. Grimbergen, P. Bennema and H. Meekes, *ActaCryst.*, 1999, **A55**, 84-94.

15 S. Fleming and A. Rohl, *Z. Kryst.*, 2005, **220**, 580-584.

16 F. R. Massaro, L. Pastero, M. Rubbo and D. Aquilano, *J. Cryst. Growth*, 2008, **310**, 706-715.

17 M. Bruno, D. Aquilano, L. Pastero and M. Prencipe, *Cryst. Growth Des.*, 2008, **8**, 2163-2170.

18 M. Bruno, F. R. Massaro and M. Prencipe, *Surf. Science*, 2008, **602**, 2774-2782.

19 M. Bruno, D. Aquilano and M. Prencipe, *Cryst. Growth Des.*, 2009, **9**, 1912-1916.

20 M. Bruno, F. R. Massaro, M. Prencipe and D. Aquilano, *CrystEngComm.*, 2010,**12**, 3626-3633.

21 L. Pastero, F. R. Massaro and D. Aquilano, *Cryst. Growth Des.*, 2007, **7**, 2749-2755.

22 F. R. Massaro, L. Pastero, E. Costa, G. Sgualdino and D. Aquilano, *Cryst. Growth Des.*, 2008, **8,** 2041-2046.

23 E. Bittarello, F. R. Massaro, M. Rubbo and D. Aquilano, *Cryst. Growth Des.*, 2009, **9**, 971-977.

24 M. Bruno, F. R. Massaro, M. Rubbo, M. Prencipe and D. Aquilano, *Cryst. Growth Des.*, 2010,**10**, 3102-3109**.**

25 M. Rubbo, M. Bruno and D. Aquilano, *Cryst. Growth Des.*, 2011, **11**, 2351-2357.

26 M. Rubbo, M. Bruno, F. R. Massaro and D. Aquilano, *Cryst. Growth Des.*, 2012, **12**, 264-270.

27 M. Rubbo, M. Bruno, F.R. Massaro and D. Aquilano, *Cryst. Growth Des.*, 2012, **12**, 3018-3024.

28 M. Rubbo, M. Bruno, F. R. Massaro and D. Aquilano, *CrystEngComm.*, 2013, **15**, 958-964.

29 (a) G. Wulff, *Z. Krist*., 1901**, 34** , 449-530; (b) R. Kern, in: *Morphologyof Crystals*, I. Sunagawa Ed., 1987, Terra Sci. Publish. Co. Tokyo, 77-206.

30 A. L. Rohl, K. Wright and J. D. Gale, *Am. Miner.,* 2003, **88**, 921-925.

31 J. D. Gale, *J. Chem. Soc. Faraday Trans.*,1997, **93**, 629-637.

32 R. Dovesi, B. Civalleri, R. Orlando, C. Roetti and V.R. Saunders, in *Reviews in Computational Chemistry*; B. K. Lipkowitz, R. Larter and T. R. Cundari, Eds.; John Wiley and Sons Inc.: New York, 2005; **Vol. 21**, 1-125.

33 D. Aquilano, M. Calleri, E. Natoli, M. Rubbo and G. Sgualdino, *Mater. Chem. Phys*., 2000, **66,**159-163.

34 D. Aquilano, M. Bruno, F. R. Massaro and M. Rubbo, *Cryst. Growth Des.,*2011, **11**, 3985-3993.

35 L. Pastero, D. Aquilano, E. Costa and M. Rubbo, *J. Cryst. Growth*, 2005, **275**, e1625-e1630.

36 (a) B. Evans, R. Wright, W. Haskins, A. Laakso, PIRA Conf., Fillers and Pigments for Papermakers, 2005, Atlanta, GA; (b) E. J. Osterhuber, M. G. McFadden, N. Roman, Int. Paper & Coating Chem. Symp. Proceedings, 1996, pp 47-55; (c) E. C. Silva Souto, J. J. Ribeiro Damasceno, C. E. Hori, *Materials Science Forum*, 2008, **591-593**, 526-530.

37 J. D. Gale, *General Utility Lattice Program (GULP) User's Manual*, Curtin University of Technology, Perth, Australia.

38 F. R. Massaro, M. Bruno and D. Aquilano, *Cryst. Growth Des.*, 2010, **10**, 4096-4100.

39 (a) J. Aizenberg, A. J. Black and G. M. Withesides, *Nature,*1999, **398**, 495-498; (b) S. Champ, A. Dickinson, P. S. Fallon, B. R. Heywood and M. Mascal, *Angew. Chem.*, 2000,**112**, 2828-2831; (c) A. M. Travaille, J. J. J. M. Donners, J. W. Gerritsen, N. A. J. M. Sommerdijk, R. J. M. Nolte and H. van Kempen, *Adv. Mater.*, 2002, **14**, 492-495; (d) S. Champ, A. Dickinson, P.S. Fallon, B.R. Heywood and M. Mascal, *Angew. Chem. Int. Ed.*, 2000, **39**, 2716-2719; (e) D. Volmer, M. Fricke, C. Agena and J. Mattay, *J. Mater. Chem.,* 2004, **14**, 2249-2259; (f) J. Aizenberg, A. J. Black and G. M. Withesides, *J. Amer. Chem. Soc.*, 1999, **121**, 4500-4509; (g) D. D. Archibald, S. B. Qadri and P. B. Gaber, *Langmuir*, 1996, **12**, 538-546; (h) A. Barman, D. J. Ahn, A. Lio, M. Salmeron, A. Reichert and D. Charych, *Science,* 1995, **269**, 515-518.

Figure captions

Figure 1. The growth shape of calcite, calculated according to the BFDH criterion which does not allow to distinguish between positive {$hk.l$} and negative {$hk.\bar{l}$} forms. The shape is built from the ratios between the values in the fourth column of Table 1. The positive steep rhombohedron {01.2} and the negative one {01.$\bar{2}$} are equally important and dominant, followed by the {00.1} pinacoid. It is worth noting that the cleavage {10.4} rhombohedron does not appear in the growth morphology.

Figure 2. The un-relaxed and relaxed profiles of the main positive and negative forms of calcite. Drawings represent, for a given crystallographic form, only the profile associated to the minimum specific surface energy.

Figure 3. Calculated relaxed Equilibrium Shape of calcite: {10.4} cleavage and {01.2} steep rhombohedron; {10.0} prism; {00.1} pinacoid. None of the negative forms enters the ES, but the {01.$\bar{2}$} negative steep rhombohedron that could belong to the ES under a small reduction (close to 7%) of its surface energy.

Graphical abstract
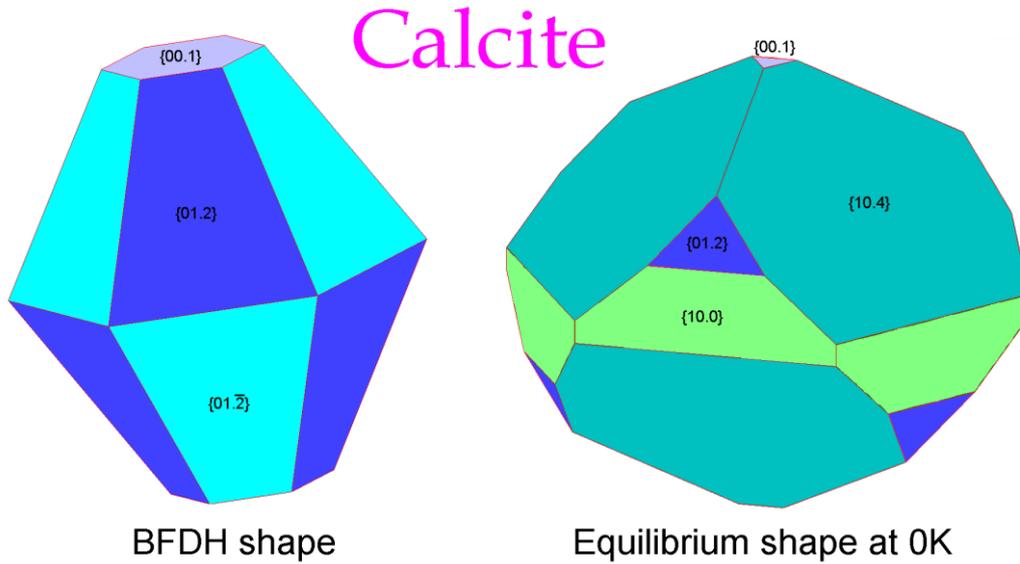
Relaxed surface profiles of the negative forms $\{10.\bar{4}\}$, $\{01.\bar{2}\}$, $\{01.\bar{8}\}$ and $\{21.\bar{4}\}$ of calcite are compared to those of the well-known positive ones: $\{10.4\}$, $\{01.2\}$, $\{01.8\}$ and $\{21.4\}$. Throughthe approach of the PBC analysis, by Hartman-Perdok, the optimal surfaces are obtained for the calculation of the surface energies.The cleavage $\{10.4\}$ form is the very reference of the crystal, while the $\{01.2\}$ and $\{01.\bar{2}\}$ forms have unexpectedly close surface energy values and compete for entering the crystal equilibrium shape. The results are compared with those obtained, for the growth shape, by applying the Bravais–Friedel–Donnay –Harker's reticular approach which appears unfit to interpret the properties of crystalsurfaces.